DETECTION OF GAMMA-RAY EMISSION FROM THE STARBURST GALAXIES M82 AND NGC 253 WITH THE LARGE AREA TELESCOPE ON *FERMI*

A. A. Abdo[1,2], M. Ackermann[3], M. Ajello[3], W. B. Atwood[4], M. Axelsson[5,6], L. Baldini[7], J. Ballet[8], G. Barbiellini[9,10], D. Bastieri[11,12], K. Bechtol[3], R. Bellazzini[7], B. Berenji[3], E. D. Bloom[3], E. Bonamente[13,14], A. W. Borgland[3], J. Bregeon[7], A. Brez[7], M. Brigida[15,16], P. Bruel[17], T. H. Burnett[18], G. A. Caliandro[15,16], R. A. Cameron[3], P. A. Caraveo[19], J. M. Casandjian[8], E. Cavazzuti[20], C. Cecchi[13,14], Ö. Çelik[21,22,23], E. Charles[3], A. Chekhtman[1,24], C. C. Cheung[21], J. Chiang[3], S. Ciprini[13,14], R. Claus[3], J. Cohen-Tanugi[25], J. Conrad[6,26,27,53], C. D. Dermer[1], A. de Angelis[28], F. de Palma[15,16], S. W. Digel[3], E. do Couto e Silva[3], P. S. Drell[3], A. Drlica-Wagner[3], R. Dubois[3], D. Dumora[29,30], C. Farnier[25], C. Favuzzi[15,16], S. J. Fegan[17], W. B. Focke[3], L. Foschini[31], M. Frailis[28], Y. Fukazawa[32], S. Funk[3], P. Fusco[15,16], F. Gargano[16], D. Gasparrini[20], N. Gehrels[21,33], S. Germani[13,14], B. Giebels[17], N. Giglietto[15,16], F. Giordano[15,16], T. Glanzman[3], G. Godfrey[3], I. A. Grenier[8], M.-H. Grondin[29,30], J. E. Grove[1], L. Guillemot[29,30], S. Guiriec[34], Y. Hanabata[32], A. K. Harding[21], M. Hayashida[3], E. Hays[21], R. E. Hughes[35], G. Jóhannesson[3], A. S. Johnson[3], R. P. Johnson[4], W. N. Johnson[1], T. Kamae[3], H. Katagiri[32], J. Kataoka[36,37], N. Kawai[36,38], M. Kerr[18], J. Knödlseder[39], M. L. Kocian[3], M. Kuss[7], J. Lande[3], L. Latronico[7], M. Lemoine-Goumard[29,30], F. Longo[9,10], F. Loparco[15,16], B. Lott[29,30], M. N. Lovellette[1], P. Lubrano[13,14], G. M. Madejski[3], A. Makeev[1,24], M. N. Mazziotta[16], W. McConville[21,33], J. E. McEnery[21], C. Meurer[6,26], P. F. Michelson[3], W. Mitthumsiri[3], T. Mizuno[32], A. A. Moiseev[22,33], C. Monte[15,16], M. E. Monzani[3], A. Morselli[40], I. V. Moskalenko[3], S. Murgia[3], T. Nakamori[36], P. L. Nolan[3], J. P. Norris[41], E. Nuss[25], T. Ohsugi[32], N. Omodei[7], E. Orlando[42], J. F. Ormes[41], M. Ozaki[43], D. Paneque[3], J. H. Panetta[3], D. Parent[29,30], V. Pelassa[25], M. Pepe[13,14], M. Pesce-Rollins[7], F. Piron[25], T. A. Porter[4], S. Rainò[15,16], R. Rando[11,12], M. Razzano[7], A. Reimer[3,44], O. Reimer[3,44], T. Reposeur[29,30], S. Ritz[4], A. Y. Rodriguez[45], R. W. Romani[3], M. Roth[18], F. Ryde[6,27], H. F.-W. Sadrozinski[4], A. Sander[35], P. M. Saz Parkinson[4], J. D. Scargle[46], A. Sellerholm[6,26], C. Sgrò[7], M. S. Shaw[3], D. A. Smith[29,30], P. D. Smith[35], G. Spandre[7], P. Spinelli[15,16], M. S. Strickman[1], A. W. Strong[42], D. J. Suson[47], H. Takahashi[32], T. Tanaka[3], J. B. Thayer[3], J. G. Thayer[3], D. J. Thompson[21], L. Tibaldo[8,11,12], O. Tibolla[48], D. F. Torres[45,49], G. Tosti[13,14], A. Tramacere[3,50], Y. Uchiyama[3,43], T. L. Usher[3], V. Vasileiou[21,22,23], N. Vilchez[39], V. Vitale[40,51], A. P. Waite[3], P. Wang[3], B. L. Winer[35], K. S. Wood[1], T. Ylinen[6,27,52], AND M. Ziegler[4]

[1] Space Science Division, Naval Research Laboratory, Washington, DC 20375, USA; charles.dermer@nrl.navy.mil
[2] National Research Council Research Associate, National Academy of Sciences, Washington, DC 20001, USA
[3] W. W. Hansen Experimental Physics Laboratory, Kavli Institute for Particle Astrophysics and Cosmology, Department of Physics and SLAC National Accelerator Laboratory, Stanford University, Stanford, CA 94305, USA; bechtol@stanford.edu, Olaf.Reimer@uibk.ac.at
[4] Santa Cruz Institute for Particle Physics, Department of Physics and Department of Astronomy and Astrophysics, University of California at Santa Cruz, Santa Cruz, CA 95064, USA
[5] Department of Astronomy, Stockholm University, SE-106 91 Stockholm, Sweden
[6] The Oskar Klein Centre for Cosmo Particle Physics, AlbaNova, SE-106 91 Stockholm, Sweden
[7] Istituto Nazionale di Fisica Nucleare, Sezione di Pisa, I-56127 Pisa, Italy
[8] Laboratoire AIM, CEA-IRFU/CNRS/Université Paris Diderot, Service d'Astrophysique, CEA Saclay, 91191 Gif sur Yvette, France
[9] Istituto Nazionale di Fisica Nucleare, Sezione di Trieste, I-34127 Trieste, Italy
[10] Dipartimento di Fisica, Università di Trieste, I-34127 Trieste, Italy
[11] Istituto Nazionale di Fisica Nucleare, Sezione di Padova, I-35131 Padova, Italy
[12] Dipartimento di Fisica "G. Galilei," Università di Padova, I-35131 Padova, Italy
[13] Istituto Nazionale di Fisica Nucleare, Sezione di Perugia, I-06123 Perugia, Italy
[14] Dipartimento di Fisica, Università degli Studi di Perugia, I-06123 Perugia, Italy
[15] Dipartimento di Fisica "M. Merlin" dell'Università e del Politecnico di Bari, I-70126 Bari, Italy
[16] Istituto Nazionale di Fisica Nucleare, Sezione di Bari, 70126 Bari, Italy
[17] Laboratoire Leprince-Ringuet, École polytechnique, CNRS/IN2P3, Palaiseau, France
[18] Department of Physics, University of Washington, Seattle, WA 98195-1560, USA
[19] INAF—Istituto di Astrofisica Spaziale e Fisica Cosmica, I-20133 Milano, Italy
[20] Agenzia Spaziale Italiana (ASI) Science Data Center, I-00044 Frascati (Roma), Italy
[21] NASA Goddard Space Flight Center, Greenbelt, MD 20771, USA
[22] Center for Research and Exploration in Space Science and Technology (CRESST), NASA Goddard Space Flight Center, Greenbelt, MD 20771, USA
[23] University of Maryland, Baltimore County, Baltimore, MD 21250, USA
[24] George Mason University, Fairfax, VA 22030, USA
[25] Laboratoire de Physique Théorique et Astroparticules, Université Montpellier 2, CNRS/IN2P3, Montpellier, France
[26] Department of Physics, Stockholm University, AlbaNova, SE-106 91 Stockholm, Sweden
[27] Department of Physics, Royal Institute of Technology (KTH), AlbaNova, SE-106 91 Stockholm, Sweden
[28] Dipartimento di Fisica, Università di Udine and Istituto Nazionale di Fisica Nucleare, Sezione di Trieste, Gruppo Collegato di Udine, I-33100 Udine, Italy
[29] Université de Bordeaux, Centre d'Études Nucléaires Bordeaux Gradignan, UMR 5797, Gradignan, 33175, France
[30] CNRS/IN2P3, Centre d'Études Nucléaires Bordeaux Gradignan, UMR 5797, Gradignan, 33175, France
[31] INAF Osservatorio Astronomico di Brera, I-23807 Merate, Italy
[32] Department of Physical Sciences, Hiroshima University, Higashi-Hiroshima, Hiroshima 739-8526, Japan
[33] University of Maryland, College Park, MD 20742, USA
[34] University of Alabama in Huntsville, Huntsville, AL 35899, USA
[35] Department of Physics, Center for Cosmology and Astro-Particle Physics, The Ohio State University, Columbus, OH 43210, USA
[36] Department of Physics, Tokyo Institute of Technology, Meguro City, Tokyo 152-8551, Japan
[37] Waseda University, 1-104 Totsukamachi, Shinjuku-ku, Tokyo, 169-8050, Japan
[38] Cosmic Radiation Laboratory, Institute of Physical and Chemical Research (RIKEN), Wako, Saitama 351-0198, Japan

[39] Centre d'Étude Spatiale des Rayonnements, CNRS/UPS, BP 44346, F-30128 Toulouse Cedex 4, France
[40] Istituto Nazionale di Fisica Nucleare, Sezione di Roma "Tor Vergata," I-00133 Roma, Italy
[41] Department of Physics and Astronomy, University of Denver, Denver, CO 80208, USA
[42] Max-Planck Institut für extraterrestrische Physik, 85748 Garching, Germany
[43] Institute of Space and Astronautical Science, JAXA, 3-1-1 Yoshinodai, Sagamihara, Kanagawa 229-8510, Japan
[44] Institut für Astro- und Teilchenphysik and Institut für Theoretische Physik, Leopold-Franzens-Universität Innsbruck, A-6020 Innsbruck, Austria
[45] Institut de Ciencies de l'Espai (IEEC-CSIC), Campus UAB, 08193 Barcelona, Spain; arodrig@aliga.ieec.uab.es, dtorres@ieec.uab.es
[46] Space Sciences Division, NASA Ames Research Center, Moffett Field, CA 94035-1000, USA
[47] Department of Chemistry and Physics, Purdue University Calumet, Hammond, IN 46323-2094, USA
[48] Max-Planck-Institut für Kernphysik, D-69029 Heidelberg, Germany
[49] Institució Catalana de Recerca i Estudis Avançats, Barcelona, Spain
[50] Consorzio Interuniversitario per la Fisica Spaziale (CIFS), I-10133 Torino, Italy
[51] Dipartimento di Fisica, Università di Roma "Tor Vergata," I-00133 Roma, Italy
[52] School of Pure and Applied Natural Sciences, University of Kalmar, SE-391 82 Kalmar, Sweden

ABSTRACT

We report the detection of high-energy γ-ray emission from two starburst galaxies using data obtained with the Large Area Telescope on board the *Fermi Gamma-ray Space Telescope*. Steady point-like emission above 200 MeV has been detected at significance levels of 6.8σ and 4.8σ, respectively, from sources positionally coincident with locations of the starburst galaxies M82 and NGC 253. The total fluxes of the sources are consistent with γ-ray emission originating from the interaction of cosmic rays with local interstellar gas and radiation fields and constitute evidence for a link between massive star formation and γ-ray emission in star-forming galaxies.

Key words: cosmic rays – galaxies: individual (M82, NGC 253) – gamma rays: general – radiation mechanisms: non-thermal

1. INTRODUCTION

Cosmic rays are believed to be accelerated by supernova remnant shocks that are formed when a star explodes (Ginzburg & Syrovatskii 1964; Hayakawa 1969). Observations of γ-rays from supernova remnants in the Milky Way would apparently offer the best opportunity to identify the sources of cosmic rays, but cosmic-ray diffusion throughout the Galaxy results in a bright γ-ray glow, making it difficult to attribute γ-rays to cosmic-ray electrons, protons, or ions accelerated by Galactic supernova remnants. Direct evidence for the sources of cosmic rays is therefore still lacking.

The supernova remnant paradigm for cosmic-ray origin can also be tested by measuring the γ-ray emission from star-forming galaxies. Starburst galaxies, in particular, should have larger γ-ray intensities compared to the Milky Way due to their increased star formation rates, and greater amount of gas and dust that reprocess light into the IR, and, with photons, serve as targets for γ-ray production by cosmic-ray electrons and ions. If the γ-ray production rate is sufficiently increased, star-forming galaxies will be detectable by the current generation of instruments, as early estimates (e.g., Völk et al. 1989, 1996; Akyüz et al. 1991; Paglione et al. 1996) and recent detailed models (e.g., Domingo-Santamaría & Torres 2005; Persic et al. 2008; de Cea del Pozo et al. 2009; Rephaeli et al. 2010; Lacki et al. 2009) predict.

Here, we report the detection of the starburst galaxies M82 and NGC 253 in high-energy γ-rays from observations with the Large Area Telescope (LAT) on board the *Fermi Gamma-ray Space Telescope*. A description of the analysis of the observations is given in Section 2. In Section 3, the measured spectra and fluxes are compared with predictions based on theories of cosmic-ray origin from supernovae (SNe) in star-forming galaxies.

2. OBSERVATIONS AND ANALYSIS

The LAT is a pair-conversion telescope with a precision tracker and calorimeter, a segmented anti-coincidence detector which covers the tracker array, and a programmable trigger and data acquisition system. Incoming γ-rays convert into electron–positron pairs while traversing the LAT. The directions of primary γ-rays are reconstructed using information provided by the tracker subsystem while the energies are measured via the calorimeter subsystem. The anti-coincidence detector subsystem vetoes the great majority of cosmic rays that trigger the LAT. The energy range of the LAT spans from 20 MeV to >300 GeV with an angular resolution of approximately $5°1$ at 100 MeV and narrowing to about $0°14$ at 10 GeV.[54] Full details of the instrument, onboard, and ground data processing, and other mission-oriented support are given in Atwood et al. (2009).

The LAT normally operates in a scanning mode (the "sky survey" mode) that covers the whole sky every two orbits (i.e., ∼3 hr). We use data taken in this mode from the commencement of scientific operations in 2008 early August to 2009 early July. Only events satisfying the standard low-background event selection (termed "diffuse" class events) corresponding to the P6V3 instrument response functions are used in the present analysis. These instrument response functions take into account event pile-up and accidental coincidence effects in the detector subsystems that were not considered in the pre-launch definitions (Rando 2009). The effect of Earth albedo backgrounds was greatly reduced by removing photons coming from zenith angles $<105°$ and by excluding time intervals when the Earth was

---

[54] Angular resolution is defined here as the 68% containment radius of the LAT point-spread function averaged over the instrument acceptance and including photons which convert in either the thick or thin layers of the tracker array.
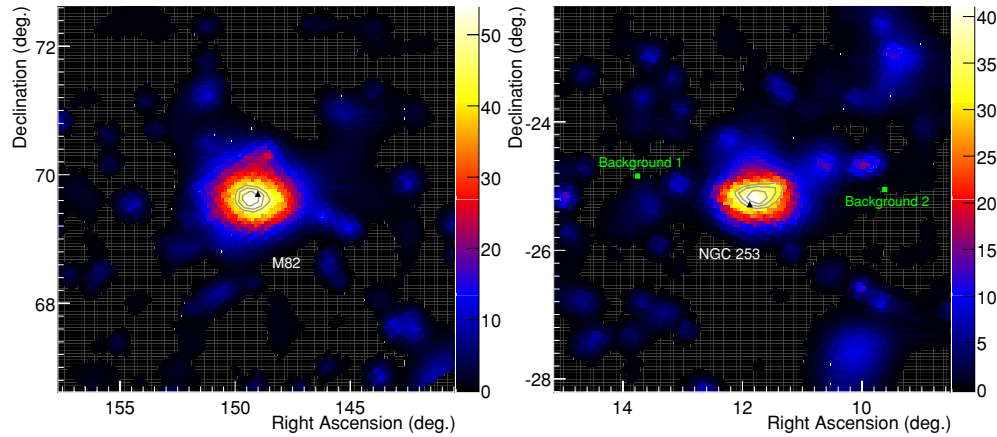
Figure 1. Test statistic maps obtained from photons above 200 MeV showing the celestial regions ($6°$ by $6°$) around M82 and NGC 253. Aside from the source associated with each galaxy, all other *Fermi*-detected sources within a $10°$ radius of the best-fit position have been included in the background model as well as components describing the diffuse Galactic and isotropic γ-ray emissions. Black triangles denote the positions of M82 and NGC 253 at optical wavelengths; gray lines indicate the 1σ, 2σ, and 3σ confidence level contours on the position of the observed γ-ray excess; green squares show the positions of individual background sources. The color scale indicates the point-source test statistic value at each location on the sky, proportional to the logarithm of the likelihood ratio between a γ-ray point-source hypothesis (L_1) vs. the background-only null hypothesis (L_0); $TS \equiv 2(\ln L_1 - \ln L_0)$ (Mattox et al. 1996).

Table 1
Results of Maximum Likelihood Analyses of M82 and NGC 253

Galaxy	R.A.[a] (deg)	Decl.[a] (deg)	r_{95}[a] (deg)	$F(>100\ \mathrm{MeV})$[b] (10^{-8} ph cm^{-2} s^{-1})	Photon Index[b]	Significance[c]
M82	149.06	69.64	0.11	$1.6 \pm 0.5_{\mathrm{stat}} \pm 0.3_{\mathrm{sys}}$	$2.2 \pm 0.2_{\mathrm{stat}} \pm 0.05_{\mathrm{sys}}$	6.8
NGC 253	11.79	-25.21	0.14	$0.6 \pm 0.4_{\mathrm{stat}} \pm 0.4_{\mathrm{sys}}$	$1.95 \pm 0.4_{\mathrm{stat}} \pm 0.05_{\mathrm{sys}}$	4.8

Notes.
[a] Source localization results (J2000) with r_{95} corresponding to the 95% confidence error radius around the best-fit position.
[b] Parameters of power-law spectral models fitted to the data: integrated photon flux >100 MeV and photon index.
[c] Detection significance of each source.

appreciably in the field of view (specifically, when the center of the field of view was more than $43°$ from the zenith).

We use all γ-rays with energy >200 MeV within a $10°$ radius region of interest of the optical locations for the galaxies M82 and NGC 253. Detection significance maps for each region are shown in Figure 1. The background model for each region includes all LAT-detected sources along with components describing the diffuse Galactic and isotropic γ-ray emissions. Each map shows a bright and isolated γ-ray excess above the background that is consistent with the location of the nominal (optical) position of the respective starburst galaxy.

We used a maximum likelihood fitting procedure (*gtlike*, version v9r15p2)[55] with the P6V3 instrument response functions described above to determine the positions of the γ-ray sources associated with M82 and NGC 253 (see Table 1). The angular separation between the best-fit location and the core of each galaxy is $0°.05$ for M82 and $0°.12$ for NGC 253. Systematic uncertainties in the positions due to inaccuracies in the point-spread function and telescope alignment are estimated to be less than $0°.01$.

We tested the possibility that the sources are spatially extended by fitting two-dimensional Gaussian-shaped intensity profiles. The widths and locations of the profiles were adjusted

---

[55] *gtlike* is part of the LAT Science Tools package available from the *Fermi* Science Support Center (http://fermi.gsfc.nasa.gov/ssc/). Additional information regarding the LAT instrument response functions, data analysis software, diffuse background models, and public data access is also available from this URL.

and refitted over the region in an iterative procedure but we found no significant evidence for source extension in our data. We verified these results using a likelihood fitting procedure capable of modeling spatially extended γ-ray sources (*sourcelike*). A comparison between the point and extended source hypotheses using this method produces negligible changes in detection significance. From our analysis we set upper limits on the angular sizes of the emitting regions as $0°.18$ for M82 and $0°.30$ for NGC 253 at the 95% confidence level assuming a two-dimensional Gaussian spatial model parameterized by the 68% surface intensity containment radius. By comparison, the angular sizes of the galaxies are $0°.19 \times 0°.07$ for M82 and $0°.46 \times 0°.11$ for NGC 253 as measured in the ultraviolet band (Gil de Paz et al. 2007). The starburst cores of M82 (Völk et al. 1996) and NGC 253 (Ulvestad 2000) have an angular extent of $<0°.01$ and cannot be resolved by the LAT.

Spectral analysis is a separate maximum likelihood calculation for which we have adopted the point-source hypothesis and best-fit position determined during the localization and extension fitting step.

Diffuse γ-ray emission from the Milky Way is treated with the Galactic diffuse model corresponding to gll_iem_v02.fit which is suitable for analysis with the LAT Science Tools. In addition to the spatially structured Galactic diffuse emission, *Fermi* also observes an isotropic diffuse component which includes both extragalactic diffuse γ-ray emission and instrumental background from charged particles triggering the LAT. The isotropic diffuse emission has been treated with isotropic_iem_v02.txt.

Table 2
Properties of γ-ray Galaxies Lacking Active Central Nuclei

Galaxy	d (Mpc)	$R_{\rm SN}$ (yr^{-1})	$M_{\rm Gas}$ ($10^9\ M_\odot$)	F_γ[a] (10^{-8} ph cm^{-2} s^{-1})	$4\pi d^2 F_\gamma$[a] (10^{42} ph s^{-1})	L_γ[a] (10^{39} erg s^{-1})
LMC[b]	0.049 ± 0.001	0.005 ± 0.002	0.67 ± 0.08	26.3 ± 4.7	0.074 ± 0.013	0.041 ± 0.007
Milky Way[c]	1	0.02 ± 0.01	6.5 ± 2.0	4.6 ± 2.3	5.5 ± 2.8	3.2 ± 1.6
M82	3.6 ± 0.3	0.2 ± 0.1	2.5 ± 0.7	1.6 ± 0.5	25 ± 9	13 ± 5.0
NGC 253	3.9 ± 0.4	0.2 ± 0.1	2.5 ± 0.6	0.6 ± 0.4	11 ± 7	7.2 ± 4.7

Notes.
[a] γ-ray fluxes, F_γ, and luminosities, L_γ, computed in the energy range 100 MeV to 5 GeV.
[b] LMC: distance measurement by Pietrzynski et al. (2009); SN rate estimated by Tammann et al. (1994); mass estimate by Bruns et al. (2005; see also Westerlund 1997); γ-ray flux from Abdo et al. (2009a).
[c] Gas mass estimate from Dame (1992); γ-ray flux from the Milky Way as viewed from a distance of 1 Mpc; γ-ray luminosity estimated using models which take into account pion-decay, inverse Compton, and bremsstrahlung photons produced in both the Galactic disk and halo (Bloemen et al. 1984; Strong et al. 2000; Pavlidou & Fields 2002).

Except for the sources associated with M82 and NGC 253, all individual objects detected by *Fermi* after 11 months of scientific operations within a $10°$ radius of the best-fit position of each galaxy are also included into the background description of each region as distinct point sources.

We considered alternative associations for the two LAT sources of interest aside from M82 and NGC 253 in the CRATES catalog of flat-spectrum radio sources (14,467 entries; Healey et al. 2007) and the Candidate Gamma-Ray Blazar Survey catalog, CGRaBS (1625 entries, Healey et al. 2008). Both of these catalogs show high correlation with γ-ray bright blazars based on multiwavelength observations. However, there are no likely CRATES or CGRaBs objects within the positional uncertainty of either LAT source. Near NGC 253, the only source of possible concern is a ~40 mJy NRAO VLA Sky Survey (NVSS; Condon et al. 1998) radio source at 1.4 GHz with unknown spectrum. Such a source would be unusually weak by comparison with the radio fluxes of LAT blazars.

For each γ-ray source, we searched for flux variability by creating a monthly history of the photon flux >400 MeV arriving from within a circular region of $1°$ in radius centered on the *Fermi*-determined location. No flaring events are observed, and the χ^2 goodness-of-fit test is consistent with constant flux for each source (reduced $\chi^2 = 0.80$ and 1.03 for M82 and NGC 253, respectively, each with 9 degrees of freedom). Lack of variability is in accord with the cosmic-ray origin hypothesis where most of the emission derives from diffuse cosmic-ray interactions, though mild variability of γ-rays and radio emission (Kronberg et al. 2000, Brunthaler et al. 2009b) might still occur if M82 or NGC 253 had a recent supernova (SN). Large amplitude γ-ray variability on short timescales would rule out a cosmic-ray origin of the γ radiation.

Table 1 summarizes the results of the analyses of M82 and NGC 253 using the LAT Science Tools. The overall detection significance is 6.8σ for M82 and 4.8σ for NGC 253. Note that the significance level for these moderately hard spectrum sources is based on the number of high-energy photons compared to the expected background, whereas the flux uncertainty is based on the number of such photons, which is not large, and systematic effects. The integral photon fluxes over 100 MeV are calculated by extrapolation of the fitted spectral models.

3. INTERPRETATION

With the nearest luminous starburst galaxies, M82 and NGC 253, detected by the *Fermi Gamma-ray Space Telescope*,

we can test long-standing predictions based on the cosmic-ray paradigm that diffuse γ-ray emission from star-forming galaxies is produced via cosmic-ray interactions. The distance to M82 is 3.63 ± 0.34 Mpc (Freedman et al. 1994), and distance estimates to NGC 253 range from 2.5 Mpc (Turner & Ho 1985, Mauersberger et al. 1996) to 3.9 ± 0.37 Mpc (Karachentsev et al. 2003). Vigorous star formation is observed within the central several hundred parsecs of these galaxies. Estimates of the SN explosion rate vary from ≈ 0.08–0.3 yr^{-1} in M82 to ≈ 0.1–0.3 yr^{-1} in NGC 253 compared to the SN rate of ≈ 0.02 yr^{-1} in the Milky Way. Recent studies of M82 find $7 \times 10^8\ M_\odot$ in atomic H I gas and $1.8 \times 10^9\ M_\odot$ in H$_2$ gas (Casasola et al. 2004). The central region of NGC 253 contains a bar of molecular gas with an estimated mass of $4.8 \times 10^8\ M_\odot$ (Canzian et al. 1988), and its total gas content is $\approx 60\%$ of the Milky Way's (Boomsma et al. 2005; Houghton et al. 1997; Brunthaler et al. 2009a), reflecting active star formation taking place in these relatively small galaxies.

Table 2 gives adopted values of distance d, SN rate $R_{\rm SN}$, total gas mass $M_{\rm Gas}$, γ-ray flux $F(>100$ MeV), and γ-ray luminosities for M82 and NGC 253, alongside those of the Large Magellanic Cloud (LMC) and the Milky Way. The 100 MeV to 5 GeV γ-ray luminosity of M82 and NGC 253 is $\approx 10^{40}$ erg s^{-1}, compared to $\approx 3 \times 10^{39}$ erg s^{-1} for the Milky Way, and $\approx 4.1 \times 10^{38}$ erg s^{-1} for the LMC. These galaxies lack active central nuclei and so require a different origin for their γ-ray fluxes than from galaxies with supermassive black hole jets. The γ-rays from our Galaxy and the LMC arise predominantly from cosmic rays interacting with interstellar gas and radiation fields. The starburst galaxies M82 and NGC 253, though having less gas than the Milky Way, have a factor of 2–4 greater γ-ray luminosity, suggesting a connection between active star formation and enhanced cosmic-ray energy densities in star-forming galaxies.

We examine several possible correlations between total gas mass, SN rate, and γ-ray luminosity of these four galaxies as illustrated in Figure 2 (cf. Pavlidou & Fields 2001, for Local Group galaxies). In the left-hand panel, we find a poor correlation between γ-ray luminosity and gas mass, and a weak linear correlation between γ-ray luminosity and SN rate. Models that attribute the γ-rays to cosmic-ray processes depend both on enhanced cosmic-ray intensities, which depends on the SN rate, and large quantities of target gas, suggesting that the γ-ray luminosity is proportional to the product of the total SN rate and gas mass, as shown in the right-hand panel of Figure 2. Note that while the detection of galaxies in this sample is flux-limited, the
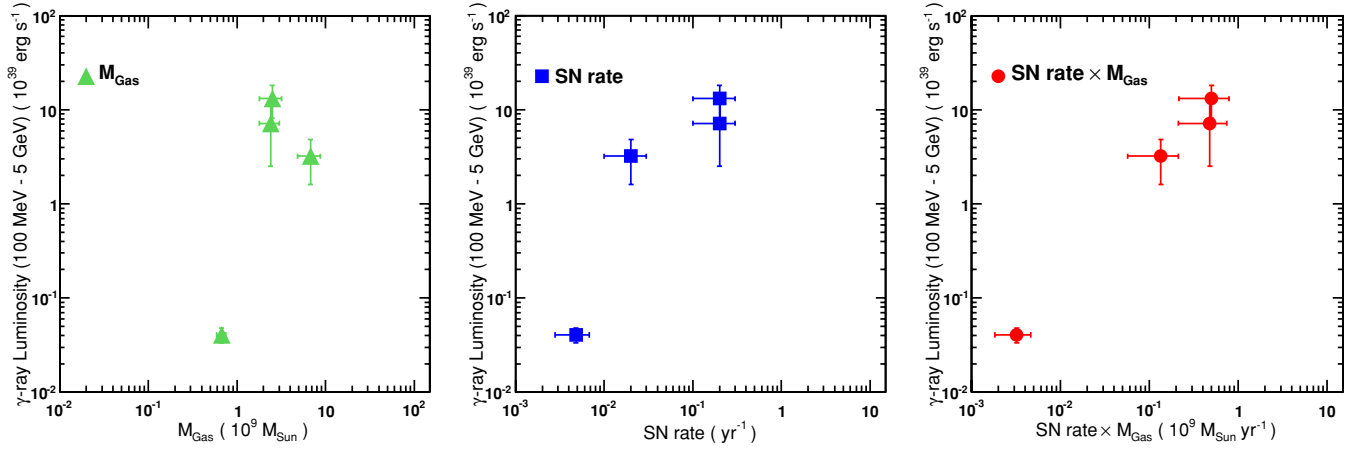
Figure 2. Relationship between SN rate, total gas mass, and total γ-ray luminosity of four galaxies detected by their diffuse high-energy emission. In order of ascending γ-ray luminosity, the plotted galaxies are the LMC, Milky Way, NGC 253, and M82. Three panels are shown to compare different possible correlations with the γ-ray luminosity: total gas mass (left), SN rate (center), and product of the total gas mass and SN rate (right). This figure is based upon the observed quantities and associated uncertainties presented in Table 2.
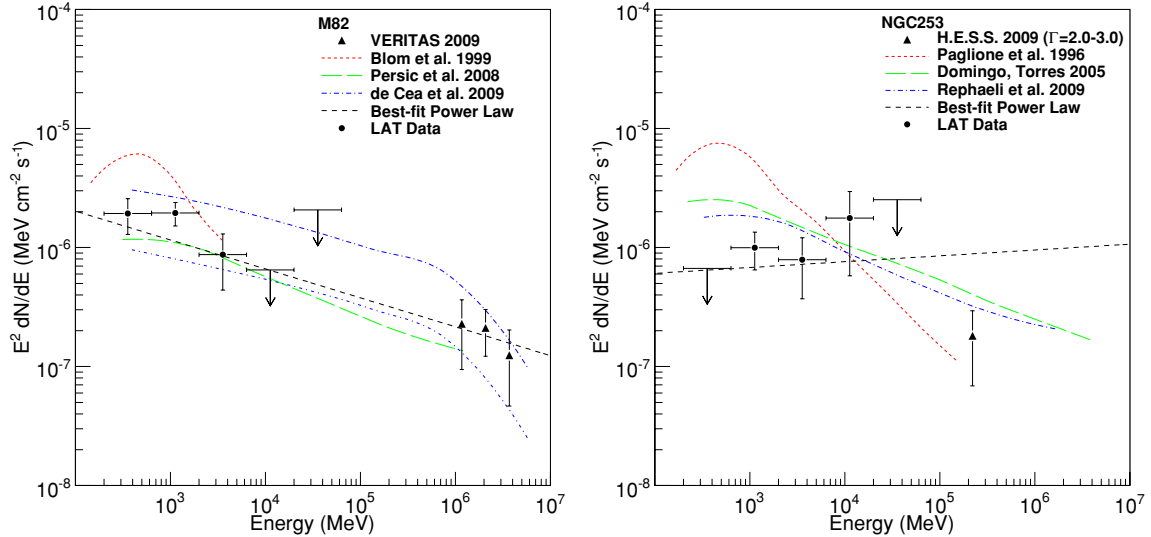
Figure 3. Spectral energy distributions of M82 and NGC 253. The spectra were obtained using a maximum likelihood analysis with flux points extracted based upon the parameters presented in Table 1. Upper limits from the LAT correspond to the 1σ confidence level. Three flux points in the TeV energy range are provided by VERITAS observations of M82 (Acciari et al. 2009). The single very high energy flux point for NGC 253 is computed from the integral photon flux >220 GeV reported by the H.E.S.S. collaboration (Acero et al. 2009) assuming a power-law spectral model with photon index between 2.0 and 3.0. Several theoretical predictions are plotted for comparison to the observed γ-ray spectra.

measured gas masses and SN rates for all galaxies are not, so that the dependence of γ-ray luminosity on these parameters reflect underlying physical relationships rather than sensitivity effects. Although the sample size is small, this result argues in favor of a scaling of γ-ray luminosity according to expectations from the hypothesis that the emission is produced by cosmic-ray interactions.

Evaluation of the dependence of γ-ray luminosity on galaxy properties is complicated, however, by star formation rates that depend on location in the galaxy. Radio and infrared observations reveal that the starburst activity in M82 and NGC 253 takes place in a relatively small central region, radius ~ 200 pc for both M82 (Völk et al. 1996) and NGC 253 (Ulvestad 2000), so that the distribution of the cosmic rays in the galaxies is probably not uniform. In cases where γ-ray emission can be resolved, as for the Milky Way, this can be seen directly (Dragicevich et al. 1999). For instance, γ-ray emission from the LMC is mostly produced in the star-forming region 30

Doradus, and does not simply trace star formation and total gas mass (Abdo et al. 2009a).

Theoretical predictions, despite using different assumptions and treating the processes with varying levels of detail, are largely consistent with the detected integral flux of M82 (e.g., Völk et al. 1989; Akyüz et al. 1991; Persic et al. 2008; de Cea del Pozo et al. 2009) and NGC 253 (e.g. Paglione et al. 1996; Domingo-Santamaría & Torres 2005; Persic et al. 2008). Figure 3 shows the predicted and observed spectra. In the case of NGC 253, the predicted photon flux (>100 MeV) is 2.3×10^{-8} photons cm^{-2} s^{-1} (Domingo-Santamaría & Torres 2005) and 2×10^{-8} photons cm^{-2} s^{-1} (Persic et al. 2008). For M82, the predicted photon flux (>100 MeV) is between 2.6×10^{-8} and 8.3×10^{-9} photons cm^{-2} s^{-1} (de Cea del Pozo et al. 2009) due to systematic uncertainties in model parameters, and $\approx 10^{-8}$ photons cm^{-2} s^{-1} (Persic et al. 2008). Furthermore, extrapolation of the best-fit power-law spectral model at GeV energies provides a smooth connection to flux densities of

M82 reported at TeV energies (Acciari et al. 2009). Although not highly constrained due to the faintness of M82 in the GeV band, the fitted spectrum suggests that a single physical emission mechanism dominates from GeV to TeV energies. The relationship between the GeV and TeV emission for NGC 253 is less clear given the current data. Also, note that the inner starburst region of NGC 253 has about a factor of 3 less radio flux than that of M82 at 1.4 GHz, consistent with the galaxy being less luminous in γ-rays (M82, Klein et al. 1988; NGC 253, Carilli 1996).

The star-forming galaxy contribution to the extragalactic γ-ray background (EGB) can be estimated by writing the EGB intensity as $\epsilon I_\epsilon^{sf} \cong R_H \zeta \rho b L_\gamma / 4\pi$, where the Hubble radius $R_H \cong 4200$ Mpc for a Hubble constant of 71 km s^{-1} Mpc^{-1}, $\zeta \sim 3$–10 is a cosmological factor accounting for more active star formation at redshift $z \gtrsim 1$, and $\rho = \rho_3/(1000 \text{ Mpc}^3)$ is the local space density of normal and star-forming galaxies. The factor $b \cong 0.4$ corrects for the intensity at 100 MeV given the >100 MeV luminosity. Writing $L_\gamma = 10^{40} L_{40}$ erg s^{-1} gives $\epsilon I_\epsilon^{sf} \cong 3.5 \times 10^{-10} b \zeta \rho_3 L_{40}$ erg cm^{-2} s^{-1} sr^{-1}. For L_* galaxies like the Milky Way, $\rho_3 \cong 3$–10, and for starburst galaxies like M82 and NGC 253, ρ_3 is an order of magnitude smaller (e.g., Scoville 1992). At 100 MeV, a diffuse intensity of $\epsilon I_\epsilon^{EGB}(100 \text{ MeV}) \cong 2.4 \times 10^{-9}$ erg cm^{-2} s^{-1} sr^{-1} was measured with EGRET (Sreekumar et al. 1998), similar to the *Fermi* value at 100 MeV (Abdo et al. 2009b). Inserting values for L_γ from Table 2, one finds that star-forming and starburst galaxies could make a significant, $\gtrsim 10\%$ contribution to the EGB at 100 MeV, as previously suggested (Pavlidou & Fields 2002; Thompson et al. 2007).

Observations with the *Fermi Gamma-ray Space Telescope* provide evidence that GeV emission has been detected from the starburst galaxy M82, and weaker though still significant evidence for detection of NGC 253. The *Fermi* LAT detections of these galaxies at GeV energies, together with the recent discovery of >700 GeV γ-rays from M82 with VERITAS (Acciari et al. 2009) and >220 GeV γ-rays from NGC 253 with H.E.S.S. (Acero et al. 2009), introduce a new class of γ-ray sources to γ-ray astronomy. Unlike γ-ray emitting blazars and radio galaxies powered by supermassive black holes, the evidence presented here supports a cosmic-ray origin for γ-ray production in starburst galaxies. *Fermi* observations over the upcoming years will improve our knowledge of spectra, variability properties, and number of γ-ray bright starburst galaxies, which will also constitute important targets for observations with planned large Cherenkov telescope observatories CTA and AGIS.[56]

REFERENCES

Abdo, A. A., et al. 2009a, A&A, submitted
Abdo, A. A., et al. 2009b, Phys. Rev. Lett., submitted
Acciari, V. A., et al. 2009, Nature, 462, 770
Acero, F., et al. 2009, Science, 326, 1080
Akyüz, A., Brouillet, N., & Özel, M. E. 1991, A&A, 248, 419
Atwood, W. B., et al. 2009, ApJ, 697, 1071
Bloemen, J. B. G. M., Blitz, L., & Hermsen, W. 1984, ApJ, 279, 136
Boomsma, R., Oosterloo, T. A., Fraternali, F., van der Hulst, J. M., & Sancisi, R. 2005, in ASP Conf. Proc. 331, Extra-Planar Gas, ed. R. Braun (San Francisco, CA: ASP), 247
Bruns, C., et al. 2005, A&A, 432, 45
Brunthaler, A., et al. 2009a, A&A, 497, 103
Brunthaler, A., et al. 2009b, A&A, 499, L17
Canzian, B., Mundy, L. G., & Scoville, N. Z. 1988, ApJ, 333, 157
Carilli, C. L. 1996, A&A, 305, 402
Casasola, V., Bettoni, D., & Galletta, G. 2004, A&A, 422, 941
Condon, J. J., et al. 1998, AJ, 115, 1693
Dame, T. M. 1992, in Conf. AIP Conf. Proc. 278, Back to the Galaxy, ed. S. S. Holt & F. Verter (College Park, MD: AIP), 267
de Cea del Pozo, E., Torres, D. F., & Rodriguez Marrero, A. Y. 2009, ApJ, 698, 1054
Domingo-Santamaría, E., & Torres, D. F. 2005, A&A, 444, 403
Dragicevich, P. M., et al. 1999, MNRAS, 302, 693
Freedman, W. L., et al. 1994, ApJ, 427, 628
Gil de Paz, A., et al. 2007, ApJS, 173, 185
Ginzburg, V. L., & Syrovatskii, S. I. 1964, The Origin of Cosmic Rays (New York: Macmillan)
Hayakawa, S. 1969, Cosmic Ray Physics. Nuclear and Astrophysical Aspects (New York: Wiley-Interscience)
Healey, S. E., Romani, R. W., Taylor, G. B., Sadler, E. M., Ricci, R., Murphy, T., Ulvestad, J. S., & Winn, J. N. 2007, ApJS, 171, 61
Healey, S. E., et al. 2008, ApJS, 175, 97
Houghton, S., et al. 1997, A&A, 325, 923
Karachentsev, I. D., et al. 2003, A&A, 404, 93
Klein, U., Wielebinski, R., & Morsi, H. W. 1988, A&A, 190, 41
Kronberg, P. P., Sramek, R. A., Birk, G. T., Dufton, Q. W., Clarke, T. E., & Allen, M. L. 2000, ApJ, 535, 706
Lacki, B. C., Thompson, T. A., & Quataert, E. 2009, ApJ, submitted (arXiv:0907.4161)
Mattox, J. R., et al. 1996, ApJ, 461, 396
Mauersberger, R., Henkel, C., Wiebelinski, R., Wiklind, T., & Reuter, H. P. 1996, A&A, 305, 421
Paglione, T. A. D., et al. 1996, ApJ, 460, 295
Pavlidou, V., & Fields, B. D. 2001, ApJ, 558, 63
Pavlidou, V., & Fields, B. D. 2002, ApJ, 575, L5
Persic, M., Rephaeli, Y., & Arieli, Y. 2008, A&A, 486, 143
Pietrzynski, G., et al. 2009, ApJ, 697, 862
Rando, R. 2009, arXiv:0907.0626
Rephaeli, Y., Arieli, Y., & Persic, M. 2010, MNRAS, 401, 423
Scoville, N. Z. 1992, in ASP Conf. Ser. 31, Relationships Between Active Galactic Nuclei and Starburst Galaxies, ed. A. V. Filippenko (San Francisco: ASP), 159
Sreekumar, P., et al. 1998, ApJ, 494, 523
Strong, A. W., Moskalenko, I. V., & Reimer, O. 2000, ApJ, 537, 763
Tammann, G. A., Löffler, W., & Schröder, A. 1994, ApJS, 92, 487
Thompson, T. A., Quataert, E., & Waxman, E. 2007, ApJ, 654, 219
Turner, J. L., & Ho, P. T. P. 1985, ApJ, 299, L77
Ulvestad, J. S. 2000, AJ, 120, 278
Völk, H. J., Aharonian, F. A., & Breitschwerdt, D. 1996, Space Sci. Rev., 75, 279
Völk, H. J., Klein, U., & Wielebinski, R. 1989, A&A, 213, L12
Westerlund, B. E. 1997, The Magellanic Clouds (Cambridge: Cambridge Univ. Press)

---

[56] CTA: Cherenkov Telescope Array (http://www.cta-observatory.org); AGIS: Advanced Gamma-Ray Imaging System (http://www.agis-observatory.org).